Magneto-infrared spectroscopy of Landau levels and Zeeman splitting of three-dimensional massless Dirac Fermions in $ZrTe_5$

R. Y. Chen[1,*], Z. G. Chen[2,*], X.-Y. Song[1], J. A. Schneeloch[3], G. D. Gu[3], F. Wang[1,4], N. L. Wang[1,4]

[1]*International Center for Quantum Materials, School of Physics, Peking University, Beijing 100871, China.*

[2]*National High Magnetic Field Laboratory, Tallahassee, Florida 32310, USA.*

[3]*Condensed Matter Physics and Materials Science Department, Brookhaven National Lab, Upton, New York 11973, USA.*

[4]*Collaborative Innovation Center of Quantum Matter, Beijing 100871, China.*

1 Experiments

Single crystals $ZrTe_5$ were grown from Te flux method. Detailed growth procedure was described elsewhere [1]. Magneto-reflectance measurements were performed at $T = 5$ K in a superconducting magnetic up to 17.5 Tesla in National High Magnetic Field Laboratory (NMFL) in Tallahassee. Some preliminary magneto-optical measurement below 8 Tesla were done in the laboratory of Peking university. The magnetic field is along the crystalline b-axis, i.e. perpendicular to the cleaved *ac*-surface of crystal. Infrared (IR) light from a Fourier transform spectrometer is delivered to the sample using a copper light pipe. The incident beam is parallel to the magnetic field direction

*These authors contribute equally.

with its electric field **E**//*ac*-surface of crystal, and the light reflected from the sample is detected by a composite Si bolometer. The focus of the IR light on the sample is about 1×1 mm^2.

2 Further analysis of the experimental data

In this section we perform more quantitative analysis of the experimental results presented in the main text.

From the theoretical results of Section 5 and Section 6, the optical conductivity has peaks at $\sqrt{2v_xv_yeB\hbar\cdot n+m^2}+\sqrt{2v_xv_yeB\hbar\cdot(n+1)+m^2}$ if Zeeman effects are ignored. Here v_x, v_y are Fermi velocities of the 3D Dirac fermion in the xy-plane perpendicular to the magnetic field B, m is the Dirac mass (see Section 3).

To remove the noises in the raw data of $R(B)/R(0)$, we smooth the results by taking simple moving average of 41 adjacent raw data points (within frequency range of ±9.64 cm^{-1}). The raw data and smoothed results for $B=2$T are shown in Fig. 1. The peak positions are then identified by the local maxima of the smoothed data as 202, 480, 628, 748, 856, 937 cm^{-1}.

We perform two (non-linear) least square fittings for the peak positions: (i) assuming $m=0$, we obtain that $\sqrt{v_xv_y}=4.844(\pm0.008)\times10^5$ (m/s); (ii) without assuming $m=0$, we obtain the average xy-plane Fermi velocity $\sqrt{v_xv_y}=4.843(\pm0.009)\times10^5$ (m/s) and a vanishingly small

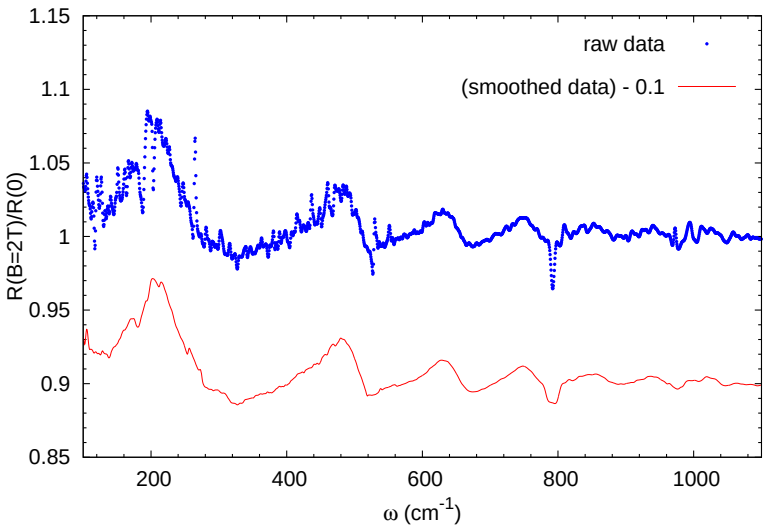

Figure 1: **Raw and smoothed data of $R(B = 2\mathbf{T})/R(0)$.** The smoothed data are obtained by simple moving average within frequency range of ± 9.64 cm^{-1}, and are shifted downward by 0.1 for clarity.

Dirac mass $|m| = 1.8(\pm 3.0)$ (cm^{-1}). Both fitting are of very high quality, as indicated by the small estimated errorbar of the average velocity. It should however be noted that the estimated errorbars do not contain uncertainties of measured peak positions. The average xy-plane Fermi velocity from our fitting is about 50% (30%) smaller than the measured Fermi velocity v_x (v_y) in an early ARPES experiment[1].

3 Low energy Hamiltonian of $ZrTe_5$

In this section we will determine the low energy effective $\boldsymbol{k} \cdot \boldsymbol{p}$ Hamiltonian for $ZrTe_5$ based on symmetry considerations.

basis states	m_{xz}	m_{yz}	$\mathcal{P}$
$\lvert\tau^z=+1, S^z=+\frac{1}{2}\rangle \equiv \lvert+,\uparrow\rangle$ $\lvert\tau^z=+1, S^z=-\frac{1}{2}\rangle \equiv \lvert+,\downarrow\rangle$	-1	$+1$	$+1$
$\lvert\tau^z=-1, S^z=+\frac{1}{2}\rangle \equiv \lvert-,\uparrow\rangle$ $\lvert\tau^z=-1, S^z=-\frac{1}{2}\rangle \equiv \lvert-,\downarrow\rangle$	$+1$	$+1$	-1

Table 1: The four basis states for the $\boldsymbol{k}\cdot\boldsymbol{p}$ theory and their symmetry quantum numbers. $\tau^z=\pm1$ labels the two Kramer pairs("orbitals"). S^z is the spin component along z-direction (crystal b-direction). m_{xz} and m_{yz} are mirror reflections about xz and yz planes respectively. $\mathcal{P}$ is spatial inversion.

From the density functional theory calculation of $ZrTe_5$ by Weng *et al.*[2], the low energy electronic excitations of this material are located around the Γ point in momentum space, and compose of certain combinations of Te p_y-orbitals. Throughout the rest of this Supplementary Information we will adopt the coordination system of Weng *et al.*, in which the x, y, z-axes correspond to crystal a, c, b-axes respectively.

The symmetry of this material contains mirror reflections m_{xz} about xz-plane, m_{yz} about yz-plane, and spatial inversion $\mathcal{P}$, and time-reversal symmetry $\mathcal{T}$. The four low energy states at Γ point are two Kramer pairs. We label each Kramer pair as "orbital" $\tau^z=\pm1$ respectively. Their symmetry quantum numbers are listed in Table 1.

The $\boldsymbol{k}\cdot\boldsymbol{p}$ Hamiltonian can in general be written as $\sum_{\boldsymbol{k}}\Psi^\dagger_{\boldsymbol{k}}\cdot H(\boldsymbol{k})\cdot\Psi_{\boldsymbol{k}}$, where $\Psi^\dagger_{\boldsymbol{k}}=$

$(c^\dagger_{\boldsymbol{k},+,\uparrow}, c^\dagger_{\boldsymbol{k},+,\downarrow}, c^\dagger_{\boldsymbol{k},-,\uparrow}, c^\dagger_{\boldsymbol{k},-,\downarrow})$, and $c^\dagger_{\boldsymbol{k},\tau^z,S^z}$ is the creation operator for basis state $|\tau^z = \pm 1, S^z = \pm\frac{1}{2}\rangle$ with wavevector $\boldsymbol{k}$, $H(\boldsymbol{k})$ is a 4×4 hermitian matrix.

The point group and time-reversal symmetries will impose strong constraints on $H(\boldsymbol{k})$. The four symmetry generators act on electrons as

$$m_{xz}: \quad \Psi_{(k_x,k_y,k_z)} \to -\tau^z \cdot \mathrm{i}\sigma^y \cdot \Psi_{(k_x,-k_y,k_z)}, \tag{1a}$$

$$m_{yz}: \quad \Psi_{(k_x,k_y,k_z)} \to \mathrm{i}\sigma^x \cdot \Psi_{(-k_x,k_y,k_z)}, \tag{1b}$$

$$I: \quad \Psi_{(k_x,k_y,k_z)} \to \tau^z \cdot \Psi_{(-k_x,-k_y,-k_z)}, \tag{1c}$$

$$\mathcal{T}: \quad \Psi_{(k_x,k_y,k_z)} \to \mathcal{K} \cdot \mathrm{i}\sigma^y \cdot \Psi_{(-k_x,-k_y,-k_z)}. \tag{1d}$$

Here τ and σ denote Pauli matrices in the "orbital" and spin spaces respectively, $\mathcal{K}$ is the anti-unitary complex conjugation operator. Therefore we have the following relations

$$\begin{aligned} & H(k_x,k_y,k_z) = \tau^z\sigma^y \cdot H(k_x,-k_y,k_z) \cdot \tau^z\sigma^y \\ = \ & \sigma^x \cdot H(-k_x,k_y,k_z) \cdot \sigma^x = \tau^z \cdot H(-k_x,-k_y,-k_z) \cdot \tau^z \\ = \ & \sigma^y \cdot [H(-k_x,-k_y,-k_z)]^* \cdot \sigma^y. \end{aligned} \tag{2}$$

Expand $H(\boldsymbol{k})$ to linear order of $\boldsymbol{k}$, it must be of the following Dirac equation form,

$$\begin{aligned} H(\boldsymbol{k}) = \ & m\,\tau^z + \hbar \cdot (v_x\,k_x\,\tau^x\sigma^z + v_y\,k_y\,\tau^y + v_z\,k_z\,\tau^x\sigma^x), \\ \equiv \ & m\,\tau^z + \hbar \cdot (\sum_{a=x,y,z} v_a\,k_a\,\Gamma_a), \end{aligned} \tag{3}$$

where the "Fermi velocities" $v_{x,y,z}$ and the "Dirac mass" m are real parameters.

4 Zeeman effects on Dirac fermions in $ZrTe_5$.

In this section we consider only the Zeeman effect of a uniform magnetic field $\boldsymbol{B}$. The Hamiltonian is $H(\boldsymbol{k}) + H_{\text{Zeeman}}$, with the symmetry-allowed Zeeman term being $H_{\text{Zeeman}} = -\mu_B \cdot (\bar{g} \cdot \boldsymbol{S} + \delta g \cdot \tau^z \boldsymbol{S}) \cdot \boldsymbol{B}$. Here $g_\pm \equiv \bar{g} \pm \delta g$ are the Landé g-factors for $\tau^z = \pm 1$ Kramer pairs respectively, and $\boldsymbol{S} = \frac{\boldsymbol{\sigma}}{2}$ is the spin-1/2 spin operator.

We will consider the three cases with Zeeman field along principal axes. For simplicity we assume $\delta g = 0$ in the following analysis. The result shows that (i) only when the field is along y-axis (crystal c-axis), the Dirac point can split into two Weyl points separated in momentum space as normally expected[3]; (ii) for large Zeeman field along x or z directions, the Dirac point will evolve into a ring of band touching points, or "line-nodes"[3], which is perturbatively protected by mirror reflection symmetry about the plane perpendicular to field direction, and will support surface flat bands for the surface perpendicular to the Zeeman field. Some more details are listed below.

- Field along x-direction: $\boldsymbol{B} = B\boldsymbol{e}_x$.

  If $\delta g = 0$, the energy eigenvalues are $\pm\sqrt{\hbar^2 v_x^2 k_x^2 + (\sqrt{\hbar^2 v_y^2 k_y^2 + \hbar^2 v_z^2 k_z^2 + m^2} \pm \bar{g}\mu_B B/2)^2}$.

  If $|\bar{g}\mu_B B/2| > |m|$, this has line-nodes $k_x = 0$, $\hbar^2 (v_y^2 k_y^2 + v_z^2 k_z^2) = (\bar{g}\mu_B B/2)^2 - m^2$.

- Field along y-direction: $\boldsymbol{B} = B\boldsymbol{e}_y$.

  If $\delta g = 0$, the energy eigenvalues are $\pm\sqrt{\hbar^2 v_x^2 k_x^2 + \hbar^2 v_z^2 k_z^2 + (\sqrt{\hbar^2 v_y^2 k_y^2 + m^2} \pm \bar{g}\mu_B B/2)^2}$.

  If $|\bar{g}\mu_B B| > |m|$, this shows two Weyl points at $k_x = k_z = 0$, $\hbar v_y k_y = \pm\sqrt{(\bar{g}\mu_B B/2)^2 - m^2}$.

- Field along z-direction: $\boldsymbol{B} = B\boldsymbol{e}_z$.

If $\delta g = 0$, the energy eigenvalues are $\pm\sqrt{\hbar^2 v_z^2 k_z^2 + (\sqrt{\hbar^2 v_x^2 k_x^2 + \hbar^2 v_y^2 k_y^2 + m^2} \pm \bar{g}\mu_B B/2)^2}$.

If $|\bar{g}\mu_B B/2| > |m|$, this has a line-nodes $k_z = 0$, $\hbar^2 (v_x^2 k_x^2 + v_y^2 k_y^2) = (\bar{g}\mu_B B/2)^2 - m^2$.

5 Landau levels for magnetic field along z-direction (line-node scenario)

In this section we will solve the Landau level structure for the $\boldsymbol{k}\cdot\boldsymbol{p}$ model (3) of $ZrTe_5$ under uniform magnetic field. For simplicity and motivated by the experiments reported in main text, we will first consider a uniform magnetic field $\boldsymbol{B} = B\boldsymbol{e}_z$ along z-direction (crystal b-direction), which can be described by a Landau gauge vector potential $\boldsymbol{A} = (-By, 0, 0)$. By the standard minimal coupling procedure, the Hamiltonian here can be deduced from (3) as $H(-\mathrm{i}\partial_{\boldsymbol{r}} + \frac{e\boldsymbol{A}}{\hbar}) + H_{\text{Zeeman}}$.

Denote $\hat{P}_a = -\mathrm{i}\hbar\partial_a + eA_a$, where $a = x, y, z$. Then in general $[\hat{P}_a, \hat{P}_b] = -\mathrm{i}\epsilon^{abc}\hbar e B_c$. In this case we have $[\hat{P}_x, \hat{P}_y] = -\mathrm{i}\hbar eB$, $[\hat{P}_x, \hat{P}_z] = [\hat{P}_y, \hat{P}_z] = 0$. For simplicity we define $\Delta = \sqrt{|2v_x v_y e\hbar B|}$, $K = v_z\hbar k_z$, $\bar{Z} = \mu_B B\,\bar{g}/2$, and $\delta Z = \mu_B B\,\delta g/2$.

- $v_x v_y B > 0$: Define $\hat{b} = \Delta^{-1}(v_x\hat{P}_x - \mathrm{i}v_y\hat{P}_y)$. Then $[\hat{b}, \hat{b}^\dagger] = 1$.

$$H = \Delta\cdot\begin{pmatrix} 0 & 0 & \hat{b} & 0 \\ 0 & 0 & 0 & -\hat{b}^\dagger \\ \hat{b}^\dagger & 0 & 0 & 0 \\ 0 & -\hat{b} & 0 & 0 \end{pmatrix} + K\,\tau^x\sigma^x + m\,\tau^z - (\bar{Z} + \delta Z\cdot\tau^z)\cdot\sigma^z. \tag{4}$$

Denote the normalzied scalar eigenfunction of $\hat{b}^\dagger\hat{b} = n$ as ϕ_n. Consider the wavefunction of

the form $\psi = \begin{pmatrix} a_1\phi_{n-1} \\ a_2\phi_n \\ a_3\phi_n \\ a_4\phi_{n-1} \end{pmatrix}$. Then $H \cdot \psi = E\,\psi$ becomes

$$\begin{pmatrix} m-\bar{Z}-\delta Z & 0 & \Delta\sqrt{n} & K \\ 0 & m+\bar{Z}+\delta Z & K & -\Delta\sqrt{n} \\ \Delta\sqrt{n} & K & -m-\bar{Z}+\delta Z & 0 \\ K & -\Delta\sqrt{n} & 0 & -m+\bar{Z}-\delta Z \end{pmatrix} \cdot \begin{pmatrix} a_1 \\ a_2 \\ a_3 \\ a_4 \end{pmatrix} = E \begin{pmatrix} a_1 \\ a_2 \\ a_3 \\ a_4 \end{pmatrix}. \quad (5)$$

Note that when $n = 0$ we must have $a_1 = a_4 = 0$.

- $v_x v_y B < 0$: Define $\hat{b} = \Delta^{-1}(v_x\hat{P}_x + \mathrm{i}v_y\hat{P}_y)$. Then $[\hat{b}, \hat{b}^\dagger] = 1$.

$$H = \Delta \cdot \begin{pmatrix} 0 & 0 & \hat{b}^\dagger & 0 \\ 0 & 0 & 0 & -\hat{b} \\ \hat{b} & 0 & 0 & 0 \\ 0 & -\hat{b}^\dagger & 0 & 0 \end{pmatrix} + K\,\tau^x\sigma^x + m\,\tau^z - (\bar{Z} + \delta Z \cdot \tau^z)\cdot\sigma^z. \quad (6)$$

Denote the normalzied scalar eigenfunction of $\hat{b}^\dagger\hat{b} = n$ as ϕ_n. Consider the wavefunction of

the form $\psi = \begin{pmatrix} a_1\phi_n \\ a_2\phi_{n-1} \\ a_3\phi_{n-1} \\ a_4\phi_n \end{pmatrix}$. Then $H \cdot \psi = E\,\psi$ becomes

$$\begin{pmatrix} m-\bar{Z}-\delta Z & 0 & \Delta\sqrt{n} & K \\ 0 & m+\bar{Z}+\delta Z & K & -\Delta\sqrt{n} \\ \Delta\sqrt{n} & K & -m-\bar{Z}+\delta Z & 0 \\ K & -\Delta\sqrt{n} & 0 & -m+\bar{Z}-\delta Z \end{pmatrix} \cdot \begin{pmatrix} a_1 \\ a_2 \\ a_3 \\ a_4 \end{pmatrix} = E \begin{pmatrix} a_1 \\ a_2 \\ a_3 \\ a_4 \end{pmatrix}. \quad (7)$$

This equation has exactly the same form as the $v_x v_y B > 0$ case. Note however that when $n = 0$ in this case we must have $a_2 = a_3 = 0$.

The Hamiltonian commutes with $\hat{n} \equiv \hat{b}^\dagger\hat{b}$, $\hat{P}_x/\hbar = -\mathrm{i}\,\partial_x$ and $\hat{P}_z/\hbar = -\mathrm{i}\,\partial_z$. The eigenstates can be labeled by the three corresponding quantum numbers $n \geq 0$, k_x and k_z. We will omit k_x in later discussions because it does not affect energy eigenvalues. The energy levels can in general be labeled as $E_{n,s}(k_z)$, where n is an integer, $|n|$ is the eigenvalue of $\hat{b}^\dagger\hat{b}$, $s = \pm 1$ indicates that the spin is along $\pm z$-direction at $k_z = 0$. The general solution of $E_{n,s}(k_z)$ requires solving a 4th degree polynomial equation. Simple formulas of the energy eigenvalues can be obtained in several special cases listed below.

- When $n = 0$, the energy eigenvalues are ($s = \pm 1$)

$$E_{n=0,s}(k_z) = \begin{cases} -s \cdot \mathrm{sgn}(\bar{Z}+m)\sqrt{K^2 + (\bar{Z}+m)^2} + \delta Z, & v_x v_y B > 0; \\ -s \cdot \mathrm{sgn}(\bar{Z}-m)\sqrt{K^2 + (\bar{Z}-m)^2} - \delta Z, & v_x v_y B < 0. \end{cases} \quad (8)$$

For simplicity of later discussion we define $\lambda = -s \cdot \mathrm{sgn}[\bar{Z} + \mathrm{sgn}(v_x v_y B) \cdot m] = \pm 1$.

- When $n > 0$ and $\delta g = 0$, the energy eigenvalues are ($\lambda = \pm 1$, $s = \pm 1$)

$$E_{\lambda n,s}(k_z) = \lambda \cdot \sqrt{K^2 + (\sqrt{\Delta^2 n + m^2} + s \cdot \lambda \cdot \bar{Z})^2}. \tag{9}$$

  s is the $2S^z$ eigenvalue at $k_z = 0$, if $\sqrt{\Delta^2 + m^2} > |\bar{Z}|$ which we will always assume.

- When $n > 0$ and $k_z = 0$ ($K = 0$), the energy eigenvalues are ($\lambda = \pm 1$, $s = \pm 1$)

$$E_{\lambda n,s}(k_z = 0) = -s \cdot \bar{Z} + \lambda \cdot \sqrt{\Delta^2 n + (m - s \cdot \delta Z)^2}. \tag{10}$$

Without the Zeeman effect the Landau levels have doubly degenerate dispersion $E_{n,s} = \mathrm{sgn}(n)\sqrt{2 v_x v_y e B \hbar \cdot |n| + (\hbar v_z k_z)^2 + m^2}$ for $n \neq 0$, and two non-degenerate linearly dispersing $E_{0,\lambda=\pm 1} = \pm\sqrt{(\hbar v_z k_z)^2 + m^2}$ for $n = 0$. The main effects of Zeeman terms are (i) the two linearly dispersing $n = 0$ Landau levels mix and open a gap of the size $\bar{g}\,\mu_B \cdot B$; (ii) the doubly degenerate $n \neq 0$ Landau levels are split by about $\bar{g}\,\mu_B \cdot B$.

We illustrate these points by plotting the Landau level dispersions in Fig. 2, under the parameters given in main text and with a magnetic field $B = 16$T.

6 Optical conductivity

In this Section we compute the optical conductivity of $ZrTe_5$ under uniform magnetic field along z-direction, based on the model and results of the last section. Our approach follows closely the

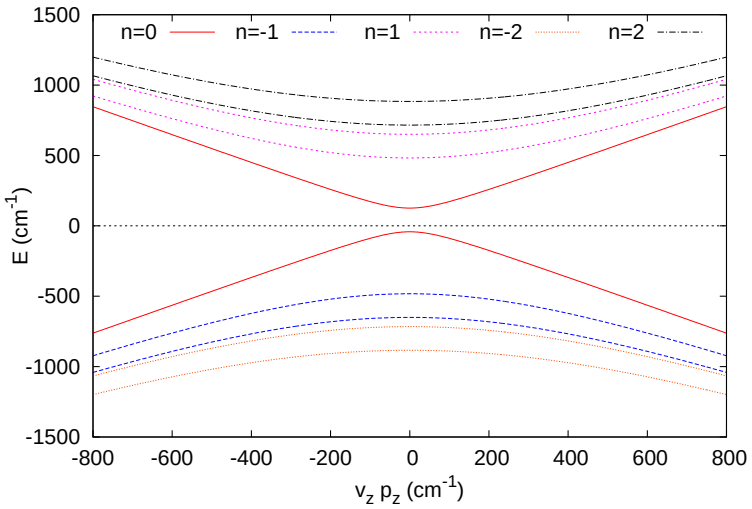

Figure 2: **Dispersion of Landau levels for field along z-direciton.** The Landau level energies versus momentum along field direction (z-direction) are displayed for Landau level index n up to $|n| = 2$. The model parameters used are $\sqrt{v_x v_y} = 4.82 \times 10^5$(m/s), $B = 16$T, $\bar{g} = 22.5$, $\delta g = \bar{g}/2$, and Dirac mass $m = 0$. Note that each $n \neq 0$ Landau level is split by about $\bar{g}\mu_B \cdot B$, and the two $n = 0$ Landau levels mix and open a gap of the size $\bar{g}\mu_B \cdot B$.

work by Ashby and Carbotte on optical conductivity of Weyl semimetals[4], but the results for this Dirac semimetal are different due to Zeeman splitting.

By Kubo formula the optical conductivity is

$$\sigma_{ab}(\omega) = -\mathrm{i}\hbar \sum_{\alpha,\beta} \frac{f(E_\alpha) - f(E_\beta)}{E_\alpha - E_\beta} \cdot \frac{\langle\alpha|\hat{j}_a|\beta\rangle\langle\beta|\hat{j}_b|\alpha\rangle}{E_\alpha - E_\beta + \hbar\omega + \mathrm{i}\delta}, \tag{11}$$

where the sum is over pairs of states α, β allowed by optical transition. The current operators are $\hat{j}_a = e\,\hat{v}_a = e \cdot \frac{\mathrm{i}}{\hbar}[\hat{H}, \hat{r}_a] = e\,v_a\,\Gamma_a$ for $a = x, y, z$.

Similar to the case of Weyl fermions[4], we have the "optical selection rule": if optical transition $\alpha \to \beta$ is allowed, states α, β must have the same k_z, their wavevector k_x (under the Landau gauge in Section 5) must be the same, if light polarization is perpendicular to the magnetic field then the Landau level indices $|n|$ of α, β must differ by 1, if light polarization is parallel to the magnetic field then the Landau level indices $|n|$ of α, β must be the same.

From the experimental fact that a very low magnetic field can put $ZrTe_5$ into quantum limit (see main text), we assume that the system is essentially "charge neutral". Then the occupied(unoccupied) electronic states are those with $\lambda = -1(+1)$ in previous section.

The real part of optical conductivity can be expressed as

$$\begin{aligned}
\mathrm{Re}[\sigma_{ab}(\omega)] = \frac{e\,B}{4\pi}\int \mathrm{d}k_z \sum_{n\geq 0,s,s'} \Big\{ & \\
& \frac{\langle -n,s|\hat{j}_a|n+1,s'\rangle\langle n+1,s'|\hat{j}_b|-n,s\rangle}{E_{n+1,s'}-E_{-n,s}}\cdot\delta(\hbar\omega+E_{-n,s}-E_{n+1,s'}) \\
& + \frac{\langle -n-1,s'|\hat{j}_a|n,s\rangle\langle n,s|\hat{j}_b|-n-1,s'\rangle}{E_{n,s}-E_{-n-1,s'}}\cdot\delta(\hbar\omega+E_{-n-1,s'}-E_{n,s})\Big\} \qquad (12) \\
= \frac{e\,B}{4\pi\hbar}\sum_{n\geq 0,s,s',k_z} \Big\{ & \frac{\langle -n,s|\hat{j}_a|n+1,s'\rangle\langle n+1,s'|\hat{j}_b|-n,s\rangle}{\omega\cdot|\frac{\partial}{\partial k_z}(E_{n+1,s'}-E_{-n,s})|}\Big|_{E_{n+1,s'}-E_{-n,s}=\hbar\omega} \\
& + \frac{\langle -n-1,s'|\hat{j}_a|n,s\rangle\langle n,s|\hat{j}_b|-n-1,s'\rangle}{\omega\cdot|\frac{\partial}{\partial k_z}(E_{n,s}-E_{-n-1,s'})|}\Big|_{E_{n,s}-E_{-n-1,s'}=\hbar\omega}\Big\}.
\end{aligned}$$

Here for simplicity k_z is omitted in the state and energy symbols. The last summation is over all k_z points where the energy difference matches $\hbar\omega$. When $n=0$, the choice of s index of $E_{-n,s}(E_{n,s})$ in the first(second) term should make $E_{-n,s}(E_{n,s})$ an occupied(unoccupied) state.

$\mathrm{Re}[\sigma_{ab}(\omega)]$ can have a peak when $\hbar\omega$ matches $E_{n+1,s'}(k_z=0)-E_{-n,s}(k_z=0)$ or $E_{n,s}(k_z=0)-E_{-n-1,s'}(k_z=0)$, because the joint density of state diverges at this energy. However the matrix elements of electric current in the numerator may suppress this peak. Note that indices s, s' indicate $2S^z$ quantum numbers at $k_z=0$. Only when $s=s'$ the matrix elements for σ_{xx} and σ_{yy} are non-vanishing at $k_z=0$. These considerations lead to (i) strong peaks of $\mathrm{Re}(\sigma_{xx})$ and $\mathrm{Re}(\sigma_{yy})$ at $E_{n+1,s}(k_z=0)-E_{-n,s}(k_z=0)$ and $E_{n,s}(k_z=0)-E_{-n-1,s}(k_z=0)$; (ii) weak peaks at $E_{n+1,-s}(k_z=0)-E_{-n,s}(k_z=0)$ and $E_{n,s}(k_z=0)-E_{-n-1,-s}(k_z=0)$. The peak positions are summarized in Table 2.

Assuming $m \ll |\bar{Z}| \ll \Delta$, the above results shows that (i) the $0\to 1$ or $-1\to 0$ transitions will produce two strong peaks at around $\Delta\pm\delta Z$, and two weak peaks at around $\Delta\pm\delta Z+2|\bar{Z}|$;

transitions	peak positions
$(0,s) \to (1,s')$	$\epsilon_{1,s} - \chi\ \delta Z + s\chi m, \quad s' = s,$ strong;
$s = \mathrm{sgn}(\bar{Z} + \chi m)$	$\epsilon_{1,-s} - \chi\ \delta Z + s\chi m + 2s\ \bar{Z}, \quad s' = -s,$ weak.
$(-1,s') \to (0,s)$	$\epsilon_{1,s} + \chi\ \delta Z - s\chi m, \quad s' = s,$ strong;
$s = -\mathrm{sgn}(\bar{Z} + \chi m)$	$\epsilon_{1,-s} + \chi\ \delta Z - s\chi m - 2s\ \bar{Z}, \quad s' = -s,$ weak.
$(n,s) \to (n+1,s')$	$\epsilon_{n+1,s} + \epsilon_{n,s}, \quad s' = s,$ strong;
$n > 0$	$\epsilon_{n+1,-s} + \epsilon_{n,s} + 2s\ \bar{Z}, \quad s' = -s,$ weak.
$(-n-1,s') \to (n,s)$	$\epsilon_{n+1,s} + \epsilon_{n,s}, \quad s' = s,$ strong;
$n > 0$	$\epsilon_{n+1,-s} + \epsilon_{n,s} - 2s\ \bar{Z}, \quad s' = -s,$ weak.

Table 2: Energy of the peaks in Re$[\sigma_{xx}(\omega)]$ or Re$[\sigma_{yy}(\omega)]$ for magnetic field along z-direction. Transitions $E_{-n,s} \to E_{n+1,s'}$ and $E_{-n-1,s'} \to E_{n,s}$ are considered. $\chi \equiv \mathrm{sgn}(v_x v_y B) = \pm 1$. $\epsilon_{n,s} \equiv \sqrt{\Delta^2 \cdot n + (m - s\ \delta Z)^2}$.

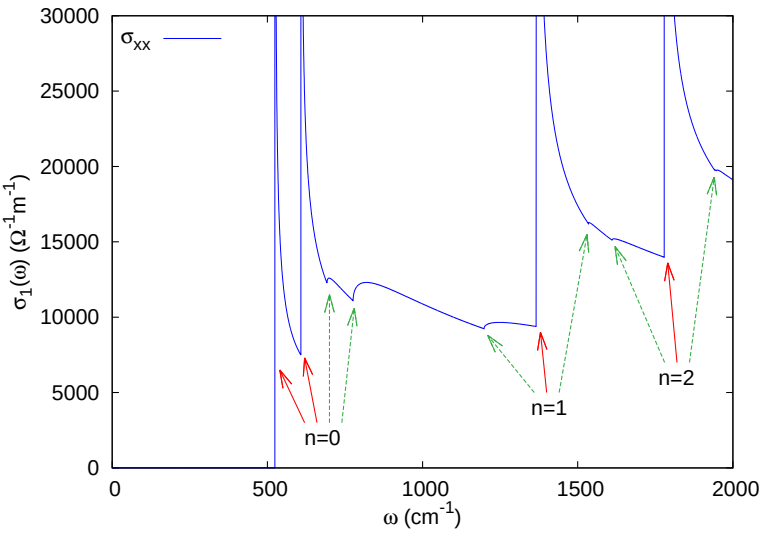

Figure 3: **Numerical results of optical conductivity for field along z-direction.** Re$[\sigma_{xx}(\omega)]$ for magnetic field $B = 16$T along z-direction. It clearly shows four peaks for the $n = 0$ ($L_0 \to L_1$ or $L_{-1} \to L_0$) transitions, and three peaks for other transitions. Strong (weak) peaks are indicated by solid red (dashed green) arrows. The model parameters used here are the same as those in Fig. 2.

(ii) the $n \to (n+1)$ or $-(n+1) \to n$ transitions will produce one strong peak at around $\Delta \cdot (\sqrt{n+1} + \sqrt{n})$. and two weak peaks at around $\Delta \cdot (\sqrt{n+1} + \sqrt{n}) \pm 2\bar{Z}$.

These conclusions are illustrated in Fig. 3, which shows the numerical results of Re$[\sigma(\omega)]$ for field $B = 16$T. It should be noted that the weak peaks for $0 \to 1$ or $-1 \to 0$ transitions are quite broad. Their apparent peak positions are actually larger than the energy values listed in Table 2. Therefore using the peak positions to fit g-factors could overestimate the g-factors.

7 Landau levels and optical conductivity for magnetic field along y-direction. (Weyl points scenario)

In this section we consider the Landau level structure and the resulting optical conductivity behavior for a uniform magnetic field B along y-direction (crystal c-direction). We are interested in this case because the Zeeman effect can split the Dirac point into two Weyl points if the orbital effect is ignored (see Section 4). We adopt Landau gauge vector potential $\boldsymbol{A} = (Bz, 0, 0)$. In this case, $[\hat{P}_z, \hat{P}_x] = -\mathrm{i}\hbar eB$ and other two commutators of the canonical momenta vanish. The Hamiltonian reads like $\hat{H} = \hbar\hat{P}_x v_x \cdot \tau^x\sigma^z + \hbar\hat{P}_y v_y \cdot \tau^y + \hbar\hat{P}_z v_z \cdot \tau^x\sigma^x + m \cdot \tau^z - \mu_B\frac{B}{2} \cdot \sigma^y(\bar{g} + \delta g \cdot \tau^z)$. For convenience in later computation, we apply a unitary transformation $\hat{U} = e^{-\mathrm{i}\sigma_x\frac{\pi}{4}}$ to the Hamiltonian which transforms σ^y into $-\sigma^z$, σ^z into σ^y and leaves σ^x invariant. For simplicity we define $\Delta = \sqrt{|2\hbar eBv_x v_z|}$, $K = v_y\hbar k_y$, $\bar{Z} = \mu_B B\bar{g}/2$, and $\delta Z = \mu_B B\delta g/2$.

- $v_x v_z B > 0$: Define $\hat{b} = \Delta^{-1}(-v_x\hat{P}_x - \mathrm{i}v_z\hat{P}_z)$. Then $[\hat{b}, \hat{b}^\dagger] = 1$.

$$H = \Delta \cdot \begin{pmatrix} 0 & 0 & 0 & \mathrm{i}\hat{b} \\ 0 & 0 & -\mathrm{i}\hat{b}^\dagger & 0 \\ 0 & \mathrm{i}\hat{b} & 0 & 0 \\ -\mathrm{i}\hat{b}^\dagger & 0 & 0 & 0 \end{pmatrix} + K\,\tau^y + m\,\tau^z + (\bar{Z} + \delta Z \cdot \tau^z) \cdot \sigma^z. \tag{13}$$

Denote the normalized scalar eigenfunction of $\hat{b}^\dagger\hat{b} = n$ as ϕ_n. Consider the wavefunction of

the form $\psi = \begin{pmatrix} a_1\phi_{n-1} \\ a_2\phi_n \\ a_3\phi_{n-1} \\ a_4\phi_n \end{pmatrix}$. Then $H \cdot \psi = E\,\psi$ becomes

$$\begin{pmatrix} m+\bar{Z}+\delta Z & 0 & -\mathrm{i}K & \mathrm{i}\Delta\sqrt{n} \\ 0 & m-\bar{Z}-\delta Z & -\mathrm{i}\Delta\sqrt{n} & -\mathrm{i}K \\ \mathrm{i}K & \mathrm{i}\Delta\sqrt{n} & -m+\bar{Z}-\delta Z & 0 \\ -\mathrm{i}\Delta\sqrt{n} & \mathrm{i}K & 0 & -m-\bar{Z}+\delta Z \end{pmatrix} \cdot \begin{pmatrix} a_1 \\ a_2 \\ a_3 \\ a_4 \end{pmatrix} = E \begin{pmatrix} a_1 \\ a_2 \\ a_3 \\ a_4 \end{pmatrix} . \quad (14)$$

Note that when $n = 0$ we must have $a_1 = a_3 = 0$.

- $v_x v_z B < 0$: Define $\hat{b} = \Delta^{-1}(-v_x\hat{P}_x + \mathrm{i}v_z\hat{P}_z)$. Then $[\hat{b}, \hat{b}^\dagger] = 1$.

$$H = \Delta \cdot \begin{pmatrix} 0 & 0 & 0 & \mathrm{i}\hat{b}^\dagger \\ 0 & 0 & -\mathrm{i}\hat{b} & 0 \\ 0 & \mathrm{i}\hat{b}^\dagger & 0 & 0 \\ -\mathrm{i}\hat{b} & 0 & 0 & 0 \end{pmatrix} + K\,\tau^y + m\,\tau^z + (\bar{Z} + \delta Z \cdot \tau^z) \cdot \sigma^z. \quad (15)$$

Denote the normalized scalar eigenfunction of $\hat{b}^\dagger\hat{b} = n$ as ϕ_n. Consider the wavefunction of

the form $\psi = \begin{pmatrix} a_1\phi_n \\ a_2\phi_{n-1} \\ a_3\phi_n \\ a_4\phi_{n-1} \end{pmatrix}$. Then $H \cdot \psi = E\,\psi$ becomes

$$\begin{pmatrix} m+\bar{Z}+\delta Z & 0 & -\mathrm{i}K & \mathrm{i}\Delta\sqrt{n} \\ 0 & m-\bar{Z}-\delta Z & -\mathrm{i}\Delta\sqrt{n} & -\mathrm{i}K \\ \mathrm{i}K & \mathrm{i}\Delta\sqrt{n} & -m+\bar{Z}-\delta Z & 0 \\ -\mathrm{i}\Delta\sqrt{n} & \mathrm{i}K & 0 & -m-\bar{Z}+\delta Z \end{pmatrix} \cdot \begin{pmatrix} a_1 \\ a_2 \\ a_3 \\ a_4 \end{pmatrix} = E \begin{pmatrix} a_1 \\ a_2 \\ a_3 \\ a_4 \end{pmatrix}. \quad (16)$$

This equation has exactly the same form as the $v_x v_z B > 0$ case. Note however that when $n = 0$ in this case we must have $a_2 = a_4 = 0$.

We ignore k_x and label the eigenstate by three quantum numbers n, s and k_y. The energy levels are $E_{n,s}(k_y)$ where s denotes the eigenvalue of $\tau^z\sigma^z$ when $K = 0$ (the Hamiltonian commutes with $\tau^z\sigma^z$ when $K = 0$). The following are some special cases for energy eigenvalues.

- When $n = 0$, the energy eigenvalues are ($s = \pm 1$)

$$E_{n=0,s}(k_y) = \begin{cases} -s \cdot \mathrm{sgn}(\delta Z - m)\sqrt{K^2 + (\delta Z - m)^2} - \bar{Z}, & v_x v_z B > 0; \\ s \cdot \mathrm{sgn}(\delta Z + m)\sqrt{K^2 + (\delta Z + m)^2} + \bar{Z}, & v_x v_z B < 0. \end{cases} \quad (17)$$

- When $n > 0$ and $\delta g = 0$, the energy eigenvalues are ($\lambda = \pm 1$, $s = \pm 1$)

$$E_{\lambda n,s}(k_z) = \lambda \cdot \sqrt{(\sqrt{m^2 + K^2} + s \cdot \bar{Z})^2 + \Delta^2 n}. \quad (18)$$

s is the $\tau^z\sigma^z$ eigenvalue at $k_y = 0$.

- When $n > 0$ and $k_y = 0$ ($K = 0$), the energy eigenvalues are ($\lambda = \pm 1$, $s = \pm 1$)

$$E_{\lambda n,s}(k_y = 0) = s \cdot \delta Z + \lambda \cdot \sqrt{\Delta^2 n + (m + s \cdot \bar{Z})^2} \tag{19}$$

The main effects of Zeeman terms are (i) the two linearly dispersing $n = 0$ Landau levels mix and open a gap of the size $\delta g \cdot \mu_B \cdot B$; (ii) the doubly degenerate $n \neq 0$ Landau levels are split by about $\delta g \cdot \mu_B \cdot B$. In the following discussion we assume δg is large enough, so that all Landau level dispersions are monotonic for $k_y \geq 0$ as shown in Fig. 4.

The optical conductivity in this case can be computed by a formula similar to equation (12), with the summation over k_z replaced by summation over k_y, and the dispersion $E_{n,s}(k_z)$ replaced by the results $E_{n,s}(k_y)$ in this section. The optical selection rule in this case is the same as the previous section. Re$[\sigma_{ab}(\omega)]$ can have a peak when $\hbar\omega$ matches $E_{n+1,s'}(k_y = 0) - E_{-n,s}(k_y = 0)$ or $E_{n,s}(k_y = 0) - E_{-n-1,s'}(k_y = 0)$, because the joint density of state diverges at this energy. However the matrix elements of electric current may suppress this peak. Note that indices s, s' indicate $\tau^z\sigma^z$ quantum numbers at $k_y = 0$. Only when $s = s'$ the matrix elements for σ_{xx} and σ_{zz} are non-vanishing for $k_y = 0$. These considerations lead to (i) strong peaks of Re(σ_{xx}) and Re(σ_{zz}) at $E_{n+1,s}(k_z = 0) - E_{-n,s}(k_z = 0)$ and $E_{n,s}(k_z = 0) - E_{-n-1,s}(k_z = 0)$; (ii) weak peaks at $E_{n+1,-s}(k_z = 0) - E_{-n,s}(k_z = 0)$ and $E_{n,s}(k_z = 0) - E_{-n-1,-s}(k_z = 0)$. The peak positions are summarized in Table 3.

Assuming $m \ll |\bar{Z}| \ll \Delta$, the above results shows that (i) the $0 \to 1$ or $-1 \to 0$ transitions will produce two strong peaks at around $\Delta \pm \bar{Z}$, and two weak peaks at around $\Delta \pm \bar{Z} + 2|\delta Z|$;

transitions	peak positions
$(0,s) \to (1,s')$	$\epsilon_{1,s} + \chi\, \bar{Z} + s\chi m, \qquad s' = s,$ strong;
$s = -\mathrm{sgn}(\delta Z - \chi m)$	$\epsilon_{1,-s} + \chi\, \bar{Z} + s\chi m - 2s\, \delta Z\,, \quad s' = -s,$ weak.
$(-1,s') \to (0,s)$	$\epsilon_{1,s} - \chi\, \bar{Z} - s\chi m, \qquad s' = s,$ strong;
$s = \mathrm{sgn}(\delta Z - \chi m)$	$\epsilon_{1,-s} - \chi\, \bar{Z} - s\chi m + 2s\, \delta Z\,, \quad s' = -s,$ weak.
$(n,s) \to (n+1,s')$	$\epsilon_{n+1,s} + \epsilon_{n,s}, \qquad s' = s,$ strong;
$n > 0$	$\epsilon_{n+1,-s} + \epsilon_{n,s} - 2s\, \delta Z\,, \quad s' = -s,$ weak.
$(-n-1,s') \to (n,s)$	$\epsilon_{n+1,s} + \epsilon_{n,s}, \qquad s' = s,$ strong;
$n > 0$	$\epsilon_{n+1,-s} + \epsilon_{n,s} + 2s\, \delta Z\,, \quad s' = -s,$ weak.

Table 3: Energy of the peaks in Re$[\sigma_{xx}(\omega)]$ or Re$[\sigma_{zz}(\omega)]$ for magnetic field along y-direction. Transitions $E_{-n,s} \to E_{n+1,s'}$ and $E_{-n-1,s'} \to E_{n,s}$ are considered. $\chi \equiv \mathrm{sgn}(v_x v_z B) = \pm 1$. $\epsilon_{n,s} \equiv \sqrt{\Delta^2 \cdot n + (m + s\, \bar{Z})^2}$.

(ii) the $n \to (n+1)$ or $-(n+1) \to n$ transitions will produce one strong peak at around $\Delta \cdot (\sqrt{n+1} + \sqrt{n})$. and two weak peaks at around $\Delta \cdot (\sqrt{n+1} + \sqrt{n}) \pm 2\delta Z$. These conclusions are illustrated in Fig. 4 and Fig. 5.

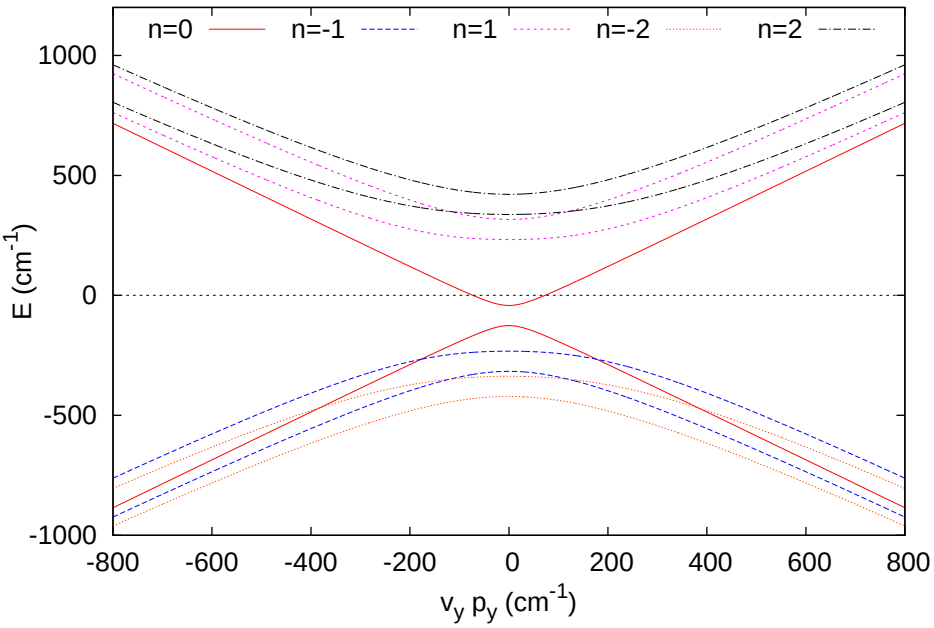

Figure 4: **Dispersion of Landau levels for field along y-direciton.** The Landau level energies versus momentum along field direction (y-direction) are displayed for Landau level index n up to $|n| = 2$. The model parameters used here are the same as those in Fig. 2.

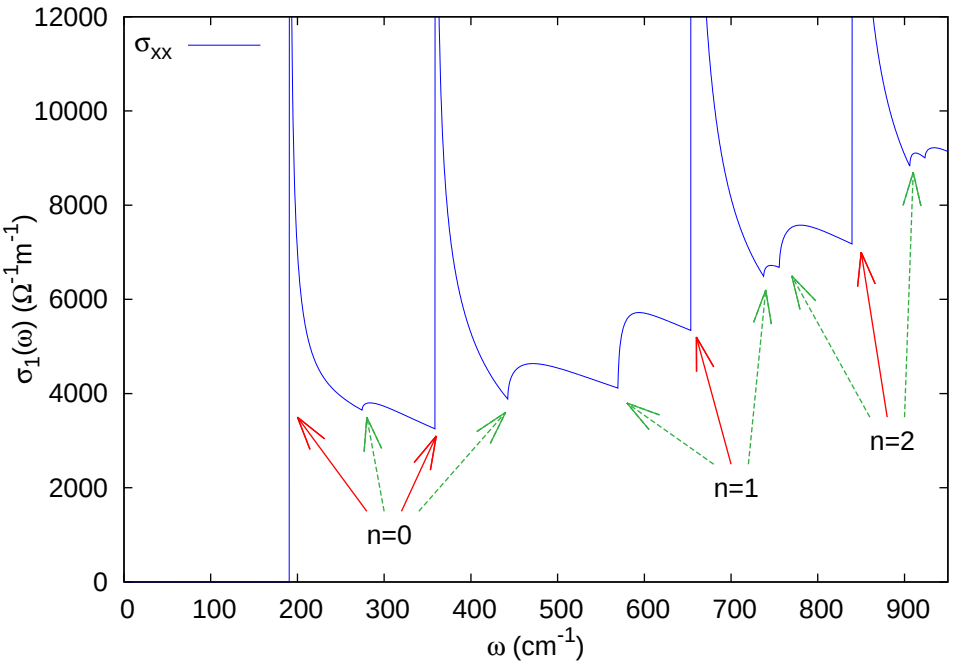

Figure 5: **Numerical results of optical conductivity for field along y-direction.** Re$[\sigma_{xx}(\omega)]$ for magnetic field $B = 16$T along y-direction. It clearly shows four peaks for the $n = 0$ transitions, and three peaks for other transitions. The model parameters used here are the same as those in Fig. 2.

1. Li, Q. *et al.* Observation of the chiral magnetic effect in $ZrTe_5$ (2014). URL http://arxiv.org/abs/1412.6543. ArXiv:1412.6543.

2. Weng, H., Dai, X. & Fang, Z. Transition-metal pentatelluride $ZrTe_5$ and $HfTe_5$: A paradigm for large-gap quantum spin hall insulators. *Phys. Rev. X* **4**, 011002 (2014). URL http://link.aps.org/doi/10.1103/PhysRevX.4.011002.

3. Burkov, A. A., Hook, M. D. & Balents, L. Topological nodal semimetals. *Phys. Rev. B* **84**, 235126 (2011). URL http://link.aps.org/doi/10.1103/PhysRevB.84.235126.

4. Ashby, P. E. C. & Carbotte, J. P. Magneto-optical conductivity of weyl semimetals. *Phys. Rev. B* **87**, 245131 (2013). URL http://link.aps.org/doi/10.1103/PhysRevB.87.245131.